INSTITUTTET FOR BYGNINGSTEKNIK
DEPT. OF BUILDING TECHNOLOGY AND STRUCTURAL ENGINEERING
AALBORG UNIVERSITET • AUC • AALBORG • DANMARK

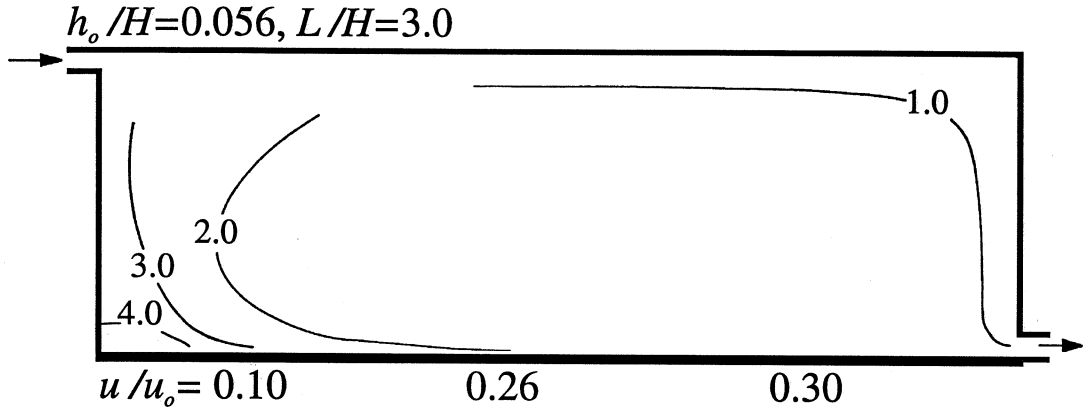

Plenary Lecture at Ventilation '94, Stockholm 1994

P. V. NIELSEN
PROSPECTS FOR COMPUTATIONAL FLUID DYNAMICS IN ROOM AIR CONTAMINANT CONTROL
DECEMBER 1994
ISSN 0902-7513 R9446

PROSPECTS FOR COMPUTATIONAL FLUID DYNAMICS IN ROOM AIR CONTAMINANT CONTROL

Peter V. Nielsen

Department of Building Technology
and Structural Engineering
Aalborg University

Introduction

The fluid dynamics research is strongly influenced by the increasing computer power which has been available for the last decades. This development is obvious from the curve in figure 1 which shows the computation cost as a function of years. It is obvious that the cost for a given job will decrease by a factor 10 every eight years.

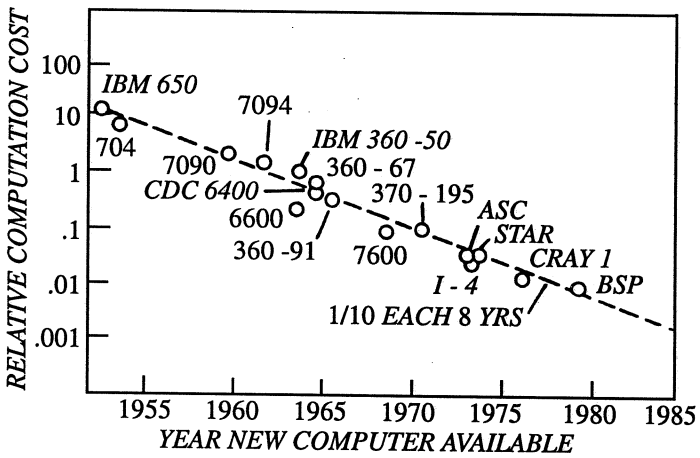

Figure 1. Trend of relative computation cost for a given flow and algorithm. Chapman (1).

The trend shows not only a decreasing cost but the computation time is also decreasing. Chapman cites an impressive example of this trend in computing efficiency, (1). He mentions that a numerical calculation of the flow over an airfoil would take 30 years if it was started in 1960 and it would cost $ 10 million. Twenty years later - in 1980 - the same calculation would take half an hour and cost $ 1000. The same calculation will not be worth mentioning today in the 'nineties.

There are various reasons for this trend. Firstly, the computer speed is increasing more rapidly than the computer cost and this tendency seems to continue. Secondly, a development takes place which increases the flexibility of different types of software as pre- and post-processor software and there is a continuous development of new software. Improvements in the fundamental routines as for example the grid generation procedure and the numerical method do also contribute to an increasing speed.

The above-mentioned tendencies have also influenced the indoor environmental technology. One of the first examples of a prediction based on Computational Fluid Dynamics (CFD) in indoor environmental technology was internationally published in 1973, (2). The activities have increased dramatically since that time and especially during the last years. It can be mentioned that all CFD papers at the first ROOMVENT conference in Stockholm in 1987 were presented within a single session, while half of all papers at the third ROOMVENT conference in Aalborg in 1992 were based on, or included, CFD calculations.

CFD is not only an important tool for the prediction of flow and contaminant distribution in ventilated spaces, it is also useful for research on local exhaust arrangements as laboratory fume hoods, paint booths, push-pull systems, canopy hoods etc.

Computational Fluid Dynamics for contaminant control is based on different equation systems as shown in the next chapter, and the chapter after that will discuss a variety of different developments of the numerical method.

A short discussion of the results from the activities sponsored by the International Energy Agency (IEA) during the period 1988 to 1991 will be mentioned and the main part of the paper will contain results from CFD prediction of contaminant transport in ventilated areas and a terminating chapter on contaminant control with local exhaust openings.

Transport equations

It is in some applications possible to consider the flow as steady, incompressible, inviscid and irrotational. This assumption can especially be made for flow which is directed against a local exhaust opening without being influenced by surfaces and changes in directions. It means that the Laplace equation applies to the flow

$$\frac{\partial^2 \phi}{\partial x^2} + \frac{\partial^2 \phi}{\partial y^2} = 0 \qquad (1)$$

where ϕ is the velocity potential and x and y are Cartesian coordinates. The flow is described as a potential flow or an ideal flow and the velocities are given as derivatives of the potential function.

The general situation with recirculating flow, velocity gradients and viscosity can be described by transport equations for mass and momentum. An equation system for steady, isothermal and incompressible flow is given by the equation of continuity

$$\frac{\partial u}{\partial x} + \frac{\partial v}{\partial y} + \frac{\partial w}{\partial z} = 0 \qquad (2)$$

and by three momentum equations

$$\rho u \frac{\partial u}{\partial x} + \rho v \frac{\partial u}{\partial y} + \rho w \frac{\partial u}{\partial z} = - \frac{\partial p}{\partial x} + 2 \frac{\partial}{\partial x} \left(\mu_{eff} \frac{\partial u}{\partial x} \right)$$

$$+\frac{\partial}{\partial y}\left(\mu_{eff}\left(\frac{\partial v}{\partial x}+\frac{\partial u}{\partial y}\right)\right)+\frac{\partial}{\partial z}\left(\mu eff\left(\frac{\partial w}{\partial x}+\frac{\partial u}{\partial z}\right)\right) \tag{3}$$

where equation (3) is valid for the x-direction. Equations (2) and (3) are time-averaged equations. u, v and w are mean velocities in three coordinate directions, p is the pressure and ρ is the density. The effective viscosity μ_{eff} is a combination of dynamic viscosity and eddy viscosity. The eddy viscosity can be considered as an additional viscosity from the turbulence and it is a reformulation of the Reynolds stresses (Boussinesq approximation). It is necessary to have further expressions for prediction of μ_{eff} as discussed at the end of this chapter.

A flow with temperature distribution may be influenced by a buoyancy effect as for example in cases with thermal plumes and stratified flow. It is in such a case necessary to extend the equations with the energy equation and to apply a buoyancy term in the vertical direction momentum equation (y-direction).

The contaminant distribution in a flow field can be found from a transport equation for mass fraction and a given velocity distribution. The velocity distribution can either be measured, predicted as potential flow (equation (1)) or be predicted from the more general equation system ((2) and (3)).

The transport equation for mass fraction is given by

$$\rho u\frac{\partial c}{\partial x}+\rho v\frac{\partial c}{\partial y}+\rho w\frac{\partial c}{\partial z}=\frac{\partial}{\partial x}\left(\frac{\mu_{eff}}{\sigma_c}\frac{\partial c}{\partial x}\right)$$

$$+\frac{\partial}{\partial y}\left(\frac{\mu_{eff}}{\sigma_c}\frac{\partial c}{\partial y}\right)+\frac{\partial}{\partial z}\left(\frac{\mu_{eff}}{\sigma_c}\frac{\partial c}{\partial z}\right)+S_c \tag{4}$$

where c can be mass fraction of a gas or mass fraction of particles or droplet number density, see (3). σ_c is the turbulent Schmidt number and S_c is a source term which is different from zero in areas where contaminant is supplied to or extracted from the flow.

The concentration of a gas (mass fraction) is often low in indoor environment and, therefore, it is not necessary to take account of the density of the gas in the generally well-mixed flow, but it may be necessary to consider the effect close to some types of emission sources.

Equation (4) is only valid for particles or droplets which are so small that the settling velocity can be ignored in comparison with the air velocities in the room. The transport of large particles can be found from the equation

$$\rho u\frac{\partial c}{\partial x}+\rho\left(v+v_s\right)\frac{\partial c}{\partial y}+\rho w\frac{\partial c}{\partial z}=\frac{\partial}{\partial x}\left(\frac{\mu_{eff}}{\sigma_c}\frac{\partial c}{\partial x}\right)$$

$$+\frac{\partial}{\partial y}\left(\frac{\mu_{eff}}{\sigma_c}\frac{\partial c}{\partial y}\right)+\frac{\partial}{\partial z}\left(\frac{\mu_{eff}}{\sigma_c}\frac{\partial c}{\partial z}\right)+S_c \tag{5}$$

where v_s is the settling velocity and S_c is a source term which also can be a

correction term which takes account of coagulation etc., see Murakami et al. (4). Equations (4) and (5) are treating the particles and the fluid carrier as continuous media (an Eulerian approach).

It might be necessary to describe a particle contaminant source as a distribution of particle sizes with initial velocity different from the local air velocity. A typical example of this situation is the particle distribution and particle trajectory from a grinding wheel. The particle inertia is important in this and in other situations and this makes it necessary to work with a model where the particles are treated individually through solution of a particle motion equation.

Lu, Fontaine and Aubertin (5) give the following simplified equations which govern the motion of a spherical particle (inertia equals drag and gravity forces).

$$\rho_p \frac{d\vec{V}}{dt} = -\frac{3}{4}\frac{\rho}{d_p} C_D (\vec{V} - \vec{U}) |\vec{U} - \vec{V}| + (\rho_p - \rho)\vec{g} \qquad (6)$$

and

$$\frac{d\vec{X}}{dt} = \vec{V} \qquad (7)$$

$\vec{V}$ and $\vec{U}$ are instantaneous particle and fluid velocity, respectively, $\vec{X}$ is particle position, ρ_p and ρ are particle and fluid density, respectively, d_p is particle diameter, $\vec{g}$ is acceleration on account of gravity and C_D is the drag coefficient.

Equations (6) and (7) make it possible to follow a finite number of particles in a known velocity field, a Lagrangian approach and reference (5) show how the method can be used for prediction of concentration level and concentration distribution in cases which have steady particle sources.

It is necessary to have a description of the turbulence - the eddy viscosity - to close the equation system (2) and (3) as well as to obtain solutions to the transport equations of the types (4) and (5). The most simple solution is to prescribe a distribution of the eddy viscosity found from earlier experience with flow of a similar type.

A widely used method is to predict the eddy viscosity from a k-ϵ turbulence model consisting of two transport equations for turbulent kinetic energy k and dissipation of turbulent kinetic energy ϵ, see Launder et al. (6). The k-ϵ turbulence model is only valid for a fully developed turbulent flow. The flow in a room will not always be a high Reynolds number flow which is fully developed everywhere in the room, but good predictions are generally obtained in areas with a certain velocity level. Low turbulence effects can be predicted in near wall regions with for example a Launder-Sharma Low Reynolds Number model (7), but the model is not suitable in a general form for prediction of turbulence far from surfaces.

The turbulence can also be predicted with more elaborated models as e.g. the Reynolds stress model. This model will close the equation system (2) and (3) with an additional number of transport equations for the Reynolds stresses, see Leschziner (8). The Reynolds stress model is superior to the standard k-ϵ model because anisotropic effects of turbulence are taken into account. Murakami (9)

shows promising results with Reynolds stress model but continuing study and validation are needed before it can be widely used for room airflow prediction.

Large eddy simulation (LES) is another description of turbulent flow based on the hypothesis that the turbulence can be separated into large and small eddies, so that the separation between the two does not have a significant effect on the evolution of large eddies, Deardorff (10). The LES method is based on the fundamental Navier-Stokes equations and the continuity equation all filtered with respect to grid space but not to time. The equation system is closed by an expression for subgrid scale Reynolds stresses, see Murakami (9) for predictions of room air movement.

Discretization and solution of the equations

It is not possible to make a directly analytical solution of differential equations of the types (2), (3), (4) and (5). Therefore, it is necessary to reformulate the differential equations into difference equations for which solution can be found in a number of grid points by a numerical method.

The development in the numerical code - during the years - can be illustrated by the following examples based on a simple transport equation for contaminant. The equation is a one-dimensional version of (4) with constant μ_{eff}.

$$\rho u \frac{\partial c}{\partial x} = \frac{\mu_{eff}}{\sigma_c} \frac{\partial^2 c}{\partial x^2} + S \tag{8}$$

Different finite difference equations are developed in the grid distribution shown in figure 2, where P is the central grid point and h is the distance between evenly distributed points.

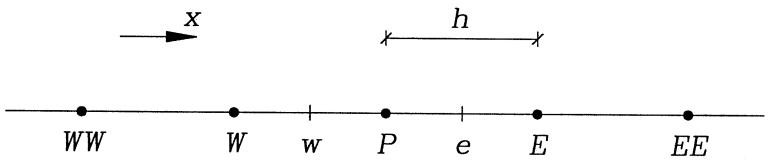

Figure 2. One-dimensional grid distribution. Grid points (capital letters) and control-volume surfaces (small letters).

A straight way to obtain a difference equation is to replace the derivatives with expressions from Taylor-series expansions, as for example

$$\left(\frac{\partial c}{\partial x}\right)_P = \frac{c_E - c_W}{2h} + 0(h^2) \tag{9}$$

$$\left(\frac{\partial^2 c}{\partial x^2}\right)_P = \frac{c_W - 2c_P + c_E}{h^2} + 0(h^2) \tag{10}$$

where $0(h^2)$ is a second-order truncation error.

The difference equation will obtain different orders of accuracy according to the accuracy of the Taylor-series expansions used. First- and second-order accuracies can be obtained for a three-point representation of equation (8) (W, P and E) and a fourth-order accuracy is obtained for a five-point representation of equation (8) (WW, W, P, E and EE).

One of the earliest attempts to obtain a numerical solution of elliptic equations like (2) to (5) with finite difference expressions like (9) and (10) was made by Thom (11) in 1933. He managed to solve the equations for Reynolds numbers up to 50.

Taylor-series formulation provides little insight into the physical meaning of the terms in the difference equation. This is, on the other hand, obtained by means of a control-volume formulation where the differential equation is integrated over a volume which is located around each grid point. The control volume in figure 2 covers the area between w to e and the one-dimensional equation (8) will have the following form in the integrated version

$$\rho u(c_e - c_w) = \frac{\mu_{eff}}{\sigma_c}\left[\left(\frac{\partial c}{\partial x}\right)_e - \left(\frac{\partial c}{\partial x}\right)_w\right] + \int_w^e S\,dx \qquad (11)$$

The most important feature is the integral conservation of quantities such as mass, momentum and energy. This feature is valid, not only for each control volume, but also for the total flow domain and it is independent of the grid distribution. Even a coarse-grid solution exhibits exact integral balances, see Patankar (12). Many commercial programmes rely on this feature and use the scheme as a sort of zonal model scheme.

A finite difference equation can be formulated from equation (11) if surface values are expressed by point values as e.g.

$$c_e = 0.5(c_E + c_P) \qquad (12)$$

the diffusion term $(\partial c/\partial x)_e$ by a central difference as (9) and the source term by $S_P h$. Other assumptions may also be used in a control-volume formulation.

Experience shows that unstable (oscillatory or wiggly) solutions are obtained in the case of an increased velocity u or increased grid point distance h. It can be shown that the Peclet number

$$Pe = \frac{h\rho u\sigma_c}{\mu_{eff}} \qquad (13)$$

must be smaller than 2 to ensure convergence and stable solutions. This is a very disadvantageous situation because most engineering applications have a high Reynolds number or a high convective flux and a small diffusion.

This situation is typical of the possibilities that were present in the 'fifties and in the 'sixties. Solutions with increasing Reynolds numbers were obtained by decreasing the distance between the grid points. On the other hand, this remedy leads in many practical situations to a number of grid points which were far too

high for computers of that time.

A large step forward was taken when Courant et al. (13) suggested the upwind scheme which gives a difference scheme with almost unconditional stability. The upwind scheme defines the values on the control-volume surface e in the convection term by

$$c_e = c_P \qquad u \geq o \tag{14 a}$$

$$c_e = c_E \qquad u < o \tag{14 b}$$

in stead of the mean value given in (12). An equivalent formulation is used at w.

In the early 'seventies it seemed that the use of upwind scheme had opened the way to making numerical simulations of flow phenomena at indefinitely high Reynold numbers. Before the end of the decade, however, it had become clear that there were errors in the predictions, although high stability was obtained. The error is connected with situations where the flow has an angle to the grid lines and it has a maximum at 45°. A "false diffusion" takes place and this diffusion is proportional to the velocity and to the distance between the grid points. Huang et al. (14) conclude that many studies at the end of the 'seventies had a false diffusion which is larger than diffusion of physical kind.

The QUICK scheme by Leonard (15) is an improved scheme for the convection term which will have a small false diffusion and a higher accuracy - second-order accuracy - in comparison with the first-order accuracy of the upwind scheme. The scheme can be interpreted as a central difference scheme with a stabilizing upstream weighted curvature correction arising from the second-order polynomial fit. The value c_e on the control-volume surface of equation (11) will have the formulation

$$c_e = \frac{1}{2}(c_E + c_P) - \frac{1}{8}(c_W - 2c_P + c_E) \qquad u \geq o \tag{15 a}$$

$$c_e = \frac{1}{2}(c_E + c_P) - \frac{1}{8}(c_P - 2c_E + c_{EE}) \qquad u < o \tag{15 b}$$

in a QUICK scheme and will replace (14 a) and (14 b) in the difference equation.

The scheme is unbounded, which means that the face value c_e can be larger than $max(c_W, c_P, c_E)$. Davidson and Fontaine (16) have shown that the scheme can improve the prediction of recirculation flow, but also that large errors may be obtained in the case of a coarse grid distribution and steep gradients.

The finite difference equations formulated from differential equations like (2) and (3) are solved by an iteration procedure. A Gauss-Seidel procedure was used earlier in the 'sixties, while a Tri-Diagonal-Matrix is used together with a line-by-line solver today, see (12).

The coupling between pressure and velocity is handled by a SIMPLE procedure. This procedure uses a staggered grid for the velocities in order to avoid unphysical oscillations in the pressure field and, furthermore, the continuity equation is rewritten into an equation for pressure correction. A detailed

description is given by Patankar (12).

Baker (17) shows the development of a finite element method in stead of the finite volume method described above and predictions for room air distribution with a finite element method are given by Baker et al. (18).

International research cooperation in room air movement

An international research programme on air distribution in rooms was sponsored by the International Energy Agency (IEA) during the period 1988 to 1991. The programme was given the name "Airflow Pattern within Buildings" and it was an important event because a number of countries joined a research cooperation in which both full-scale experiments, scale-model experiments and Computational Fluid Dynamics were performed, see reference (19).

Eleven countries joined the CFD part of this IEA project. The air movements in a room with the length, width and height equal to 4.2 m, 3.6 m and 2.5 m were predicted for isothermal flow and for non-isothermal flow with a warm window surface. The prediction was based on the continuity equation (2), the momentum equation (3) and a k-ϵ turbulence model as well as the energy equation in the case of non-isothermal flow.

Figure 3 shows the prediction of the mean velocity u_m in the occupied zone versus the air change rate in the case of isothermal flow found by the countries. Measurements of the mean velocity are also shown in the figure.

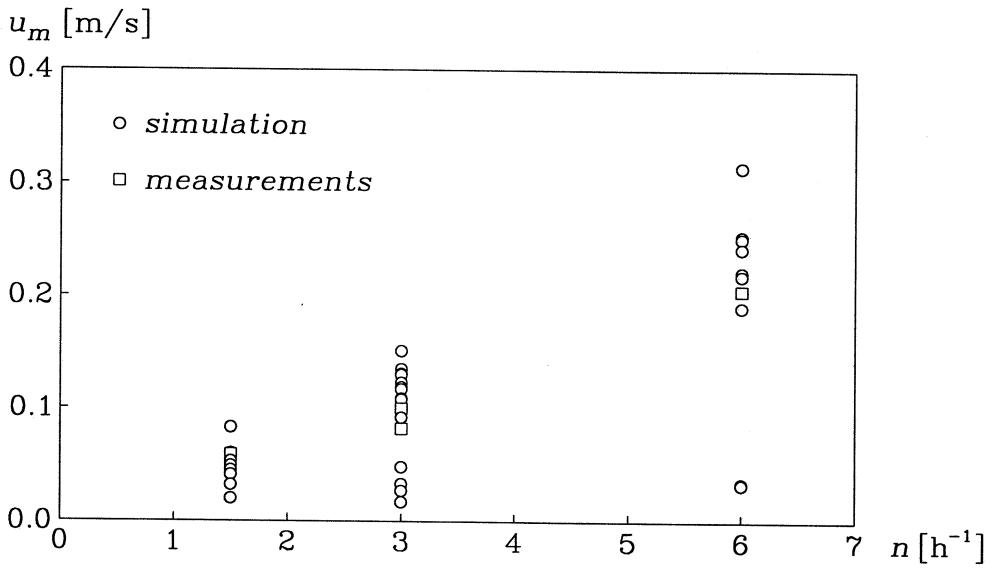

Figure 3. Mean velocity u_m versus air change rate n for the IEA project. Isothermal flow, (19, 20).

The figure shows that the results from the participating countries varied considerably. The variation may be a result of different codes, different descriptions of boundary conditions and perhaps also of different grid distributions and number of grid points. The description of boundary conditions at the inlet may be one of the important problems because the flow close to a diffuser is very complicated.

Improvements of the boundary condition at the supply opening will be one of the remedies for better predictions. Figure 4 shows the results for a Simplified Boundary Condition (SBC) where the supply area, momentum flow and direction of velocity are preserved in the boundary conditions. Comparison with measurements shows that the maximum velocity in the occupied zone is overestimated by 40%.

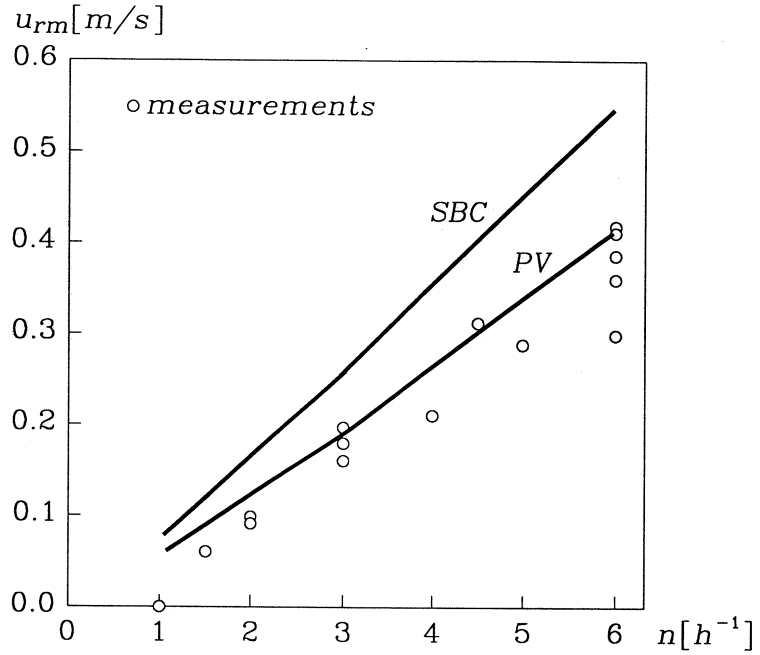

Figure 4. Maximum velocity in the occupied zone versus air change rate. Measurements and predictions in connection with the IEA, Annex 20 work. SBC: Simplified boundary conditions. PV: Prescribed velocity method. Reference (21).

Figure 4 shows that it is possible to make a large improvement of the predictions by use of a more advanced description of the boundary conditions at the supply opening. The prescribed velocity method (PV) is addressed by Nielsen in reference (22) and it is given by an analytical description of one or two of the velocity components in a small volume in front of the opening. All other variables in the volume are predicted by the numerical method.

Continuous development of the computer capacity will undoubtedly make the direct methods as e.g. local grid refinement possible in the future.

The work within the IEA-project generally concludes that two-dimensional isothermal flow is well-predicted by CFD and that skill and experience are required to use codes for practical three-dimensional situations with isothermal and non-isothermal flow.

It is difficult to deal with natural and mixed convection close to cold or warm surfaces. The k-ϵ model, whis is generally used in the IEA-project, is insufficient in the near-wall region where the local Reynolds number is very low and computed heat exchange coefficients can obtain a deviation from the measured heat exchange coefficients, Chen and Jiang (23).

The IEA-project shows that it is not always sufficient to compute only half a room under symmetrical boundary conditions because the air movement may be

unsymmetrical in full-size flow. It should also be recognized that two-dimensional flows are rare and that three-dimensional simulations may be needed to investigate characteristics of interest.

Ventilation for contaminant control in rooms

The basic idea of the general ventilation is to create a flow which will absorb the contaminant from different sources in such a way that the local concentration is low everywhere in the room. A transport of contaminant must on the other hand both involve a turbulent diffusion and a convection which will give rise to concentration gradients as it will be shown in the following chapter.

The concentration c_R in the return opening of a ventilation system is dependent on the airflow rate to the room q_o and the contaminant emission S. c_R will be given from

$$c_R = S/q_o \tag{16}$$

in the case of constant emission and steady flow.

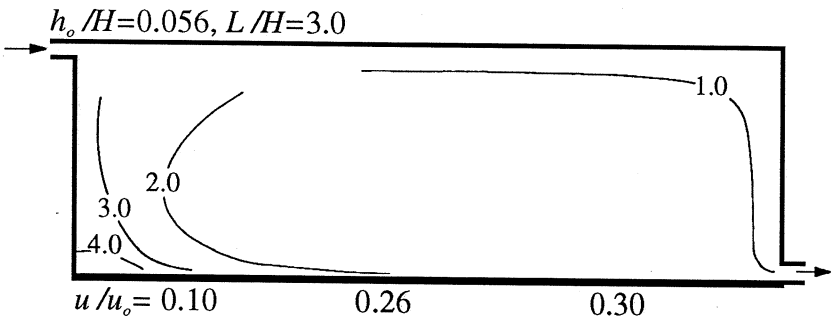

Figure 5. Concentration distribution in a room with isothermal two-dimensional flow and a contaminant source covering the whole floor. h_o, H and L are slot height, room height and room length, respectively. The velocity u is local velocity and u_o is supply velocity. Reference (24).

Figure 5 shows computer prediction of the concentration distribution in a room with a supply slot, two-dimensional isothermal flow and a contaminant source which covers the whole floor. The predictions are based on the continuity equation, the momentum equations and the convection-diffusion approach (Eulerian formulation) given by equation (4). The eddy viscosity is given by a k-ϵ model.

The local concentration in figure 5 is normalized by the concentration c_R. The concentration in the left side of the room below the supply slot is four times as large as the concentration in the return opening, so it is obvious that significant gradients in rooms with mixing ventilation will be found. A smaller supply slot, h_o/H = 0.01, will reduce the concentration to a level of two times the return concentration but it is still a significant gradient which is necessary to take into account when a system is designed.

The local velocity level u/u_o is also shown in figure 5. It is seen that low concentration is connected to high velocity and high concentration to low velocity or stagnant surroundings.

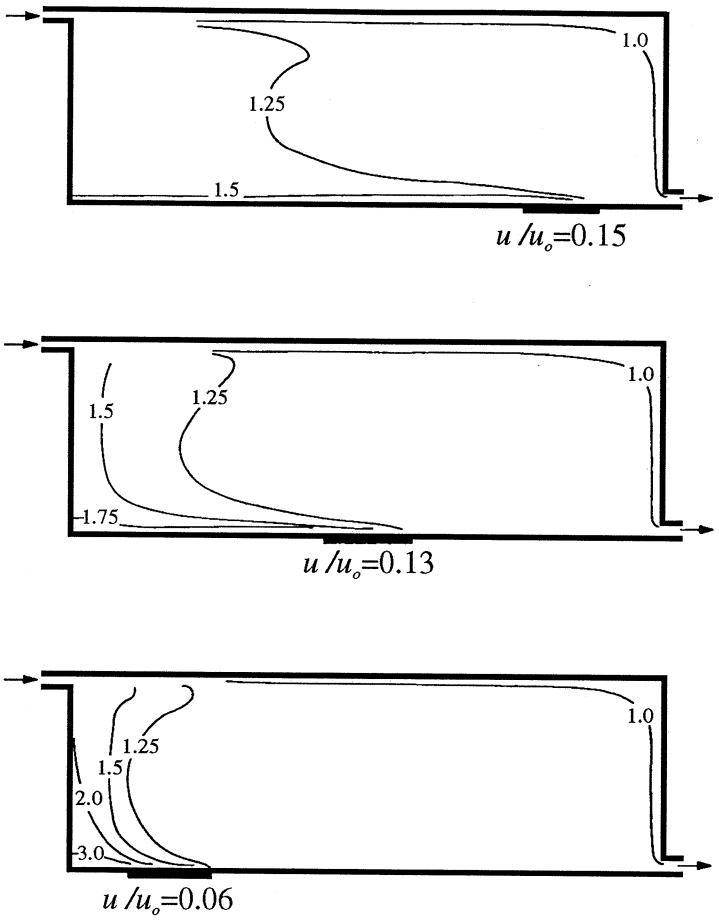

Figure 6. Concentration distribution c/c_R for different locations of a line source. Two-dimensional isothermal flow, h_o/H = 0.01 and L/H = 3.0. Reference (24).

Figure 6 shows an example of computer predicted concentration distribution from a line source. It can be seen that the location of the contaminant source is important for the concentration distribution and the concentration level. The line source is located close to the area with the maximum velocity in the occupied zone in the upper sketch. The maximum value of the concentration has a level of 1.25 - 1.5 c_R in the area below the supply slot. The concentration will increase to a level of 3.0 c_R if the source is located below the supply slot in the stagnant air as shown in the lower sketch.

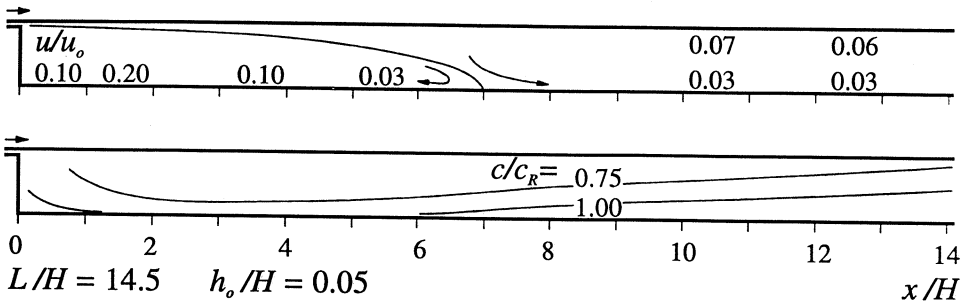

Figure 7. Velocity distribution and contaminant distribution in a deep room. Two-dimensional isothermal flow. From reference (25).

The air distribution system will cover a deep room in many old industrial buildings as shown in figure 7. The supply slot generates a plane wall jet with a penetration length - or separation length - up to 7H. This length is independent of the supply velocity u_o in the case of isothermal flow. It is shown that the maximum velocity in the occupied zone is 20% of the supply velocity and that the velocity is approximately 3% in large areas of the occupied zone.

The lower sketch in figure 7 shows the concentration distribution with an emission source which covers the whole floor. The dimensionless concentration distribution has an even distribution, but it should be considered that the dimensioned value can be very high because the exhaust concentration c_R at x/H = 14.5 contains emission from the total room length.

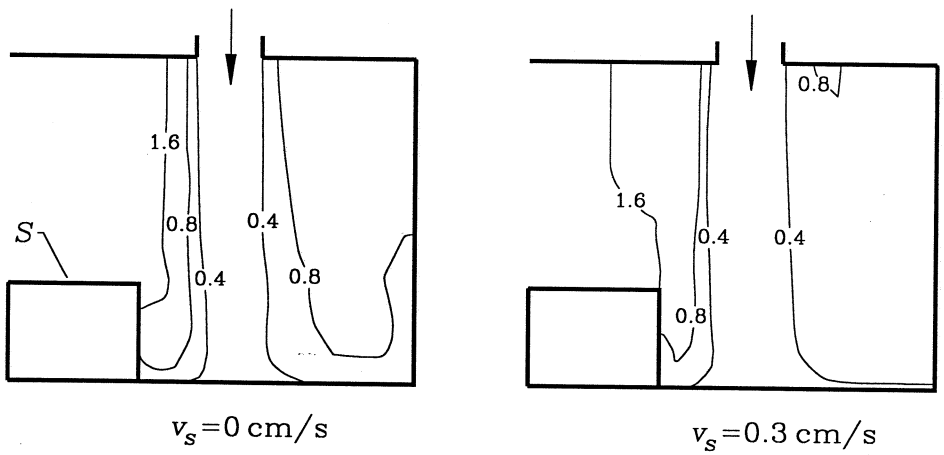

Figure 8. Predicted concentration distribution in a clean room contaminated with large particles. Murakami et al. (4).

Figure 8 shows predictions by a contaminant transport equation which takes account of particle diameter and settling velocity v_s (equation (5)). A settling velocity of zero corresponds to the conventional transport equation and the figure shows a typical contaminant distribution in a part of a clean room in this situation. The contaminant source S is located on top of the work place. Particle sizes of 10 μm give a settling velocity of 0.3 cm/s and the figure shows the

change in contaminant distribution in the room. Predictions with even larger particles (50 μm) will reduce the area with particles to a small volume above the work place and most particles will accumulate and be deposited on the work place without being exhausted from the room.

Figures 5, 6, 7, 8 show the use of CFD for a conventional prediction of concentration distribution. CFD can also be used for the predictions of parameters which are important in the evaluation of an air distribution system but very time-consuming or difficult to measure by full-scale experiments. The prediction of purging flow rate is a typical example. The purging flow rate U_p is defined as a local source divided by the obtained concentration in the control volume around the source ($U_p = S_p/c_p$).

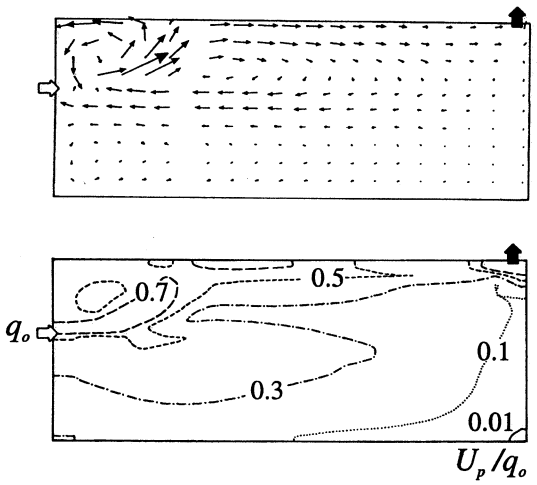

Figure 9. Velocity field and purging flow rate divided by supply flow rate. Prediction by Davidson and Olsson (26).

Figure 9 shows the velocity distribution and the distribution of purging flow rate in a room. It is obvious from the figure that a high purging flow rate is connected to areas with high velocities.

Measurement of velocity distribution and concentration distribution in rooms shows Low Reynolds Number effect, see reference (27). It is not possible to handle this effect with the turbulence models used for the predictions shown in the figures 5, 6, 7, 8 and 9 and this may cause errors at low airflow rates.

The contaminant source geometry used in the figures 5, 6 and 7 is very uncomplicated. Experiments with different contaminant sources and different geometry around the sources show that skill and experience are required in more general situations in order to obtain reliable boundary conditions for the emission.

The last example in this chapter on ventilation for contaminant control shows an exposure model by Tjelflaat (28) which can be used both on measured and predicted concentration distribution in a room. The model combines the effect of concentration level at a given position and the metabolic rate which is connected to the work made at the work place. Figure 10 illustrates the method used on a production line in a factory. The building has a volume of 4300 m^3 and it is ventilated by displacement ventilation at a rate of 30000 m^3/h. The concentration distribution is predicted in the factory and the inhaled dose of contaminant is

accumulated during a workday as a function of positions during the day and the metabolic rate of the worker.

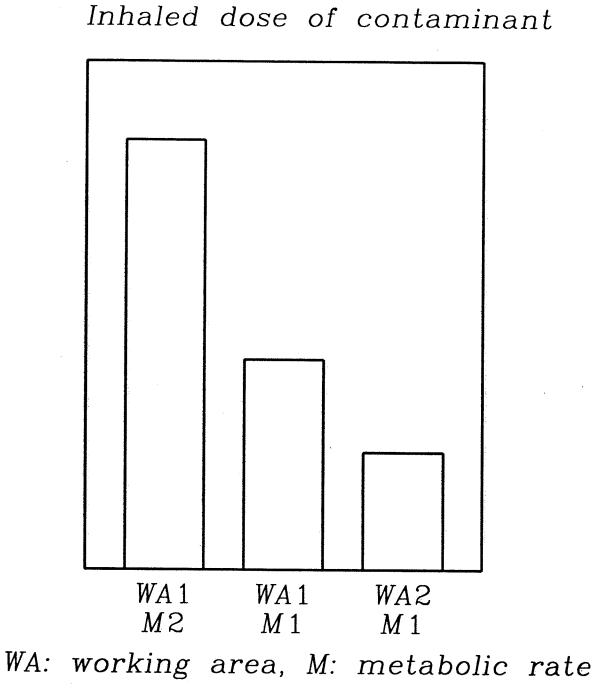

Figure 10. The accumulated inhaled dose of contaminant for one worker during a workday for three combinations of work places and worker metabolism. Tjelflaat (28).

The effect of process automation (to decrease the activity level) and the effect of transfer of the work place in order to avoid the most contaminated zones are analysed in figure 10. The original situation is the one marked WA1, M2. A lower metabolic rate in the same area, WA1, M1 will more than halve the inhaled dose rate. The position of the breathing zone, as a function of time, is the same in both cases. The transfer of the work place from the original position WA1 to a position on the opposite side of the production line WA2 gives a further reduction in the inhaled dose of contaminant.

Contaminant control with local exhaust openings

Local exhaust hoods of various configurations are used extensively in the industry to control the dispersion of harmful contaminants at the work place. Prediction of the effectiveness of a hood requires, among other things, knowledge of the air velocity field which it generates.

Research has shown that the Laplace equation (1) in terms of the velocity potential in some situations can describe the flow close to the exhaust hoods. Analytical solutions of the Laplace equation are available for infinitely flanged configurations, but it is not possible to obtain analytical solutions for unflanged hoods and other more complex configurations. A reformulation of the Laplace equation into a finite element description makes it possible to obtain a numerical prediction of the flow in many configurations as it will be shown in the following chapter.

Exhaust configuration which will generate large velocity gradients and recirculating flow can only be studied with a description containing the continuity

equation (2) and the three momentum equations (3) (Navier-Stokes equations) as well as a turbulent model for eddy viscosity.

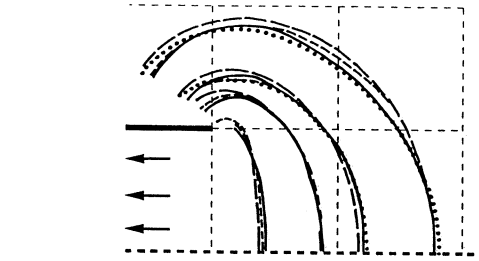

..... *Measurements*
——— *Numerical "Potential flow solution"*
------ *Numerical "Navier-Stokes solution"*

Figure 11. Velocity contour in front of an unflanged circular exhaust opening. Measurements are compared with a numerical potential flow solution and a numerical solution of Navier-Stokes equations. The contours correspond to relative velocities of 0.6, 0.3, 0.2 and 0.1.

Alenius and Jansson (29) show different numerical solutions of the flow in front of an unflanged circular exhaust opening, see figure 11. Both a numerical solution of the Laplace equation and a solution of the general flow equations agree very well with the measurements.

Figure 12 shows the velocity distribution for different configurations by a finite element modelling of the Laplace equation. Different designs of the hood with contractions or small flanges will only have an influence close to the opening. Figures A and B show that the flange on the opening generates a small modification of the plane flow around the exhaust slot, but the flow is uninfluenced some distance away from the slot. Surfaces and the wall close to the exhaust slot will influence the velocity level. A surface parallel with the slot will double the velocity level as seen in the figures A and C (principle of mirror image). A comparison of the velocity level in the figures C and D indicates that a restricted area for the potential flow will give an expected increase in velocity.

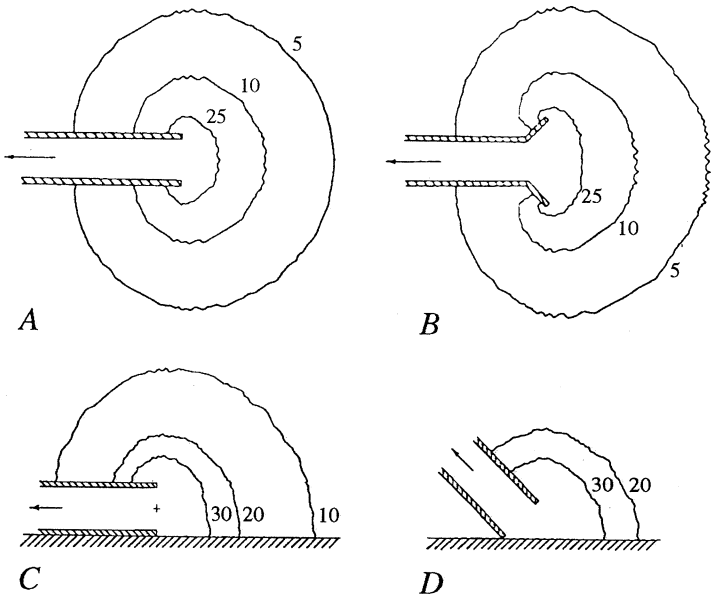

Figure 12. Velocity distribution in percentage of face velocity for different configurations of an unflanged exhaust slot. A and B show an exhaust slot far from a surface. C and D are combinations of an exhaust slot and a surface, see Garrison et al. (30).

Push-pull systems and single and double-sided exhaust systems will generate a velocity field with large velocity gradients and areas with recirculating flow. The flow must be described by an equation system which will take viscous effects and turbulence in consideration. A proper description consists of the continuity equation (2) and the momentum equations (3) as well as a k-ϵ turbulence model. The addition of a transport equation for contaminant (4) makes it possible to study the concentration distribution around the system both in undisturbed surroundings and in case of a draft around the system. Examples of predictions are given by Heinen and Zeller (31) and by Braconnier et al. (32).

An Eulerian approach based on equation (4) is used for flow of a gas and, furthermore, it can also be used for small particles. A flow of larger particles is simulated by equation (5) in cases where initial particle velocity and particle inertia can be ignored.

The Lagrangian approach is suitable for flow where initial particle velocity and particle inertia are important. Figure 13 shows a CFD prediction which illustrates the method. Figure A shows the velocity distribution close to an exhaust hood at a location with a slight cross draft. The prediction is based on the flow equations (2) and (3) and on a k-ϵ turbulence model. Figure 13 B shows a source of 60 μm particles emitted with an initial velocity of 10 m/s perpendicular to the exhaust opening. The particle velocity distribution shown in figure B is predicted from the individual particle trajectories given by equations (6) and (7). It is obvious that the initial velocity is an important factor as well as the influence of particle drag and gravity forces.

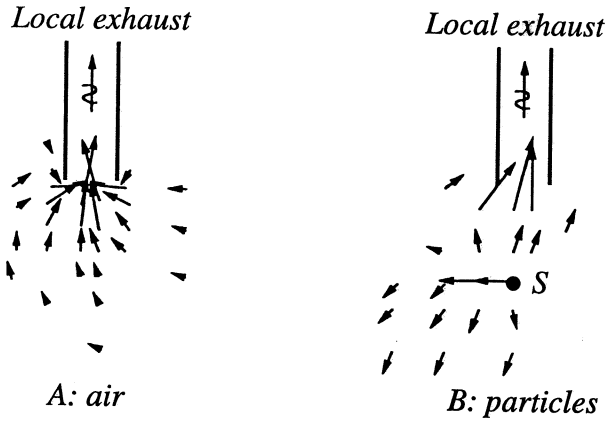

Figure 13. Flow pattern of air (A) and particles (B) in front of an exhaust opening. Madsen (33).

Fontaine et al. (34) have studied the particle flow in a fume cupboard. The front opening is a sliding door which is open for operations, see figure 14. There will be a slight recirculation of air inside the cupboard and this flow will move 30 μm particles to the upper internal exhaust slot, see figure 14A. The prediction with 70 μm particles shows that they are all moving toward the lower exhaust slot on account of the gravity effect.

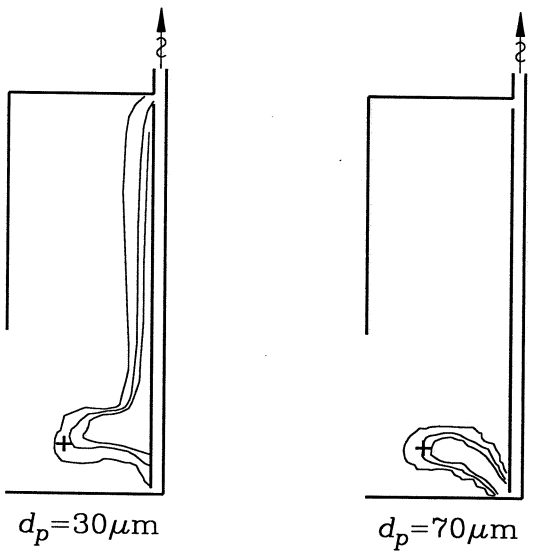

Figure 14. Computed concentration distribution in a fume cupboard in the case of a source with two different particle sizes.

The capture efficiency of an exhaust system is defined as the contaminant captured by an exhaust hood divided by the total emission of the source connected to the hood. The captured contaminant should only include gas or particles which flow directly to the exhaust hood as pointed out by Jansson (35). It is difficult to find this flow in practice, but the Lagrangian approach is an efficient method for the prediction of the flow and the capture efficiency as shown by Madsen et al. (36).

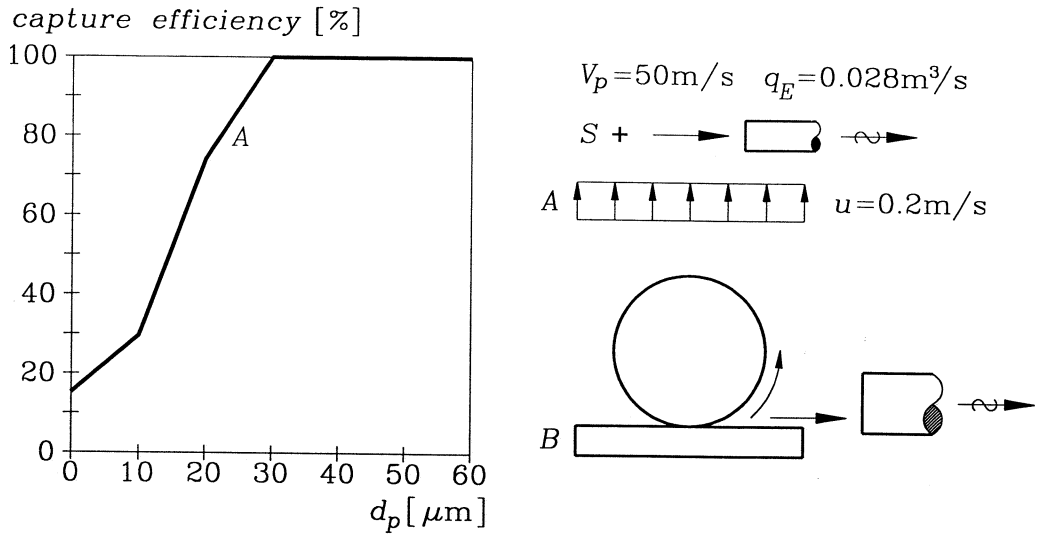

Figure 15. Capture efficiency versus particle size for the combined effect of initial particle velocity and cross draft. Madsen (33).

The last example of a Lagrangian approach is the prediction of capture efficiency for particles with initial velocity towards an opening as well as a cross draft in the area, see figure 15. Particles with a diameter larger than 30 μm are not influenced by the cross draft, while the initial momentum of the smaller particles is insufficient to make them enter the capture zone of the exhaust and the movement of the particles is governed by the cross draft. The local exhaust is therefore more efficient for large than for small particles.

Such flow situations may occur at many processes in the industry including grinding. Particles of a high momentum are emitted tangentially to the grinding wheel, whereas particles of a low momentum remain within the boundary layer until this layer is distorted by some obtacles as indicated in figure 15 B.

Conclusion

Three areas are important for the development of Computational Fluid Dynamics. These areas are the computation cost, the mathematical description of the physical processes involved in contaminant transport and, at last, the accessibility of efficient numerical methods.

It is shown that the development in computation cost has been decreasing during the last decades with a factor 10 every eight years and that the computational speed has increased rapidly during the same period.

A variety of mathematical descriptions of contaminant transport is available for different situations, but they must be selected with care in each situation.

The numerical method, including discretization and solution of the different transport equations, has also been developing during the last decades. It was only possible to make predictions for small Reynolds numbers in the 'fifties and in the 'sixties while progress in the numerical scheme makes it possible today to obtain predictions for any Reynolds number.

Special attention has been given to CFD prediction of room air motion by the IEA sponsored research "Air Flow Pattern within Building". Many countries were involved in the work with different types of CFD codes and it was generally concluded that two-dimensional isothermal flow is well-predicted and that skill

and experience are required to use codes for practical three-dimensional situations with isothermal and non-isothermal flow.

It is possible to study the use of the general ventilation system for contaminant control in rooms both in the case of contamination with gas and contamination with particles of different sizes. The information can be used for optimizing of the air distribution system. The flow will in some areas of a room be a low turbulent flow which may course some problems in predicting the exact level of concentration in that area.

Experiments with different tracer gas sources show that skill and experience are required in order to obtain reliable boundary conditions which also will be the case for CFD predictions.

Predictions of velocity and contaminant distribution close to exhaust openings agree in many cases very well with the measurements. Computational Fluid Dynamics is an efficient tool for the dimensioning of exhaust hoods of different designs and it is possible to study parameters which are difficult or time-consuming to measure.

A Lagrangrian approach with initial particle velocity at the source is a new and promising type of CFD predictions which can be used in many practical situations in the industry.

References

1. Chapman DR. Computational aerodynamics development and outlook. AIAA J., Vol. 17 (1979) 1293-1313.
2. Nielsen PV. Berechnung der Luftbewegung in einem zwangsbelüfteten Raum. Gesundheits-Ingenieur, 94, No. 10 (1973) 299-302.
3. Bradshaw P, Cebeci T and Whitelaw JH. Engineering calculation methods for turbulent flow. Academic Press, London 1981.
4. Murakami S, Kato S, Nagano S and Tanaka Y. Diffusion characteristics of airborne particles with gravitational settling in a convective-dominant indoor flow field. ASHRAE Transaction V. 98, Pt. 1 (1992) 82-97.
5. Lu QQ, Fontaine JR and Aubertin G. Particle motion in two-dimensional confined turbulent flows. Aerosol Sci. Tech. 17 (1992) 169-185.
6. Launder BE, Spalding DB and Whitelaw JH. Turbulence models and their experimental verification. Imperial College, Heat Transfer Section, Reports HTS /73/ (1973).
7. Launder BE and Sharma BI. Letters in Heat and Mass transfer. 1, 129 (1978).
8. Leschziner MA. Turbulence modelling challenges posed by complex flows. Proc. of the Third International Conference on Air Distribution in Rooms, ROOMVENT '92, Danvak, Copenhagen (1992).
9. Murakami S. Prediction, analysis and design for indoor climate in large enclosures. Proc. of the Third International Conference on Air Distribution in Rooms, ROOMVENT '92, Danvak, Copenhagen (1992).
10. Deardorff JW. A numerical study of three-dimensional turbulent channel flow at large Reynolds numbers. J. Fluid Mech., 41, (1970) 453-480.
11. Thom A. The flow past circular cylinders at low speeds. Proc. Roy. Soc., London, A 141, (1933) 651.
12. Patankar SV. Numerical heat transfer and fluid flow. Hemisphere Publishing Corporation, Washington 1980.
13. Courant R, Isaacson E and Ress M. On the solution of non-linear hyperbolic differential equations by finite differences. Comm. Pure Appl. Math. Vol. 5, (1952) 243.
14. Huang PG, Launder BE and Leschziner MA. Discretization of nonlinear convection processes: A broad-range comparison of four schemes. Comp. Methods in App. Mech. and Eng., Vol. 48, (1985) 1.
15. Leonard BP. A stable and accurate convective modelling procedure based on quadratic upstream interpolation. Comp. Methods in App. Mech. and Eng., Vol. 19, (1979) 59.

16. Davidson L and Fontaine JR. Calculation of the flow in ventilated room using different finite-difference schemes and different treatments of the walls. Proc. of CLIMA 2000, REHVA Science Series Edition, Vol 3. Amersfoort (1989) 219-225.
17. Baker AJ. Finite element computational fluid mechanics. Hermisphere Publishing Corporation, Washington 1983.
18. Baker AJ, Williams PT and Kelso RM. Development and validation of a robust CFD procedure for predicting indoor room air motion. Proc. of Indoor Air '93, Vol. 5, Helsinki (1993) 183-188.
19. Lemaire AD (Editor). Room air and contaminant flow, evaluation of computational methods. Subtask-1 Summary Report, TNO Building and Construction Research, Delft 1993.
20. Whittle GE. Evaluation of measured and computed test case results from Annex 20, subtask 1. Proc. of the 12th AIVC Conference, ISBN 0946075 53 0, AIVC, Warwick 1991.
21. Skovgaard M and Nielsen PV. Modelling complex inlet geometries in CFD - applied to air flow in ventilated rooms. Proc. of 12th AIVC Conf. ISBN 0 946075 55 7, AIVC, Warwick 1991.
22. Nielsen PV. Description of supply openings in numerical models for room air distribution. ASHRAE Transaction, Vol. 98, Part 1 (1992) 963-971.
23. Chen Q and Jiang Z. Significant questions in predicting room air motion. ASHRAE Transaction, Vol. 98, Part 1 (1992) 929-939.
24. Nielsen PV. Contaminant distribution in industrial areas with forced ventilation and two-dimensional flow. IIR-Joint Meeting, Commission E1, Essen 1981.
25. Nielsen PV. Contaminating Processes - and the general ventilation (in Danish). Aalborg University, ISSN 0902-8002 U9008, 1990.
26. Davidson L and Olsson E. Calculation of age and local purging flow rate in rooms. Building and Environment, Vol. 22, No. 2 (1987) 111-127.
27. Nielsen PV. Air distribution systems - room air movement and ventilation effectiveness. 1992 International Symposium on Room Air Convection and Ventilation Effectiveness, ASHRAE (1993) 43-52.
28. Tjelflaat PO. Evaluation of ventilation effectiveness and worker exposure at the design stage. 1992 International Symposium on Room Air Convection and Ventilation Effectiveness, ASHRAE (1993) 233-239.
29. Alenius S and Jansson A. Air flow and particle transport into local exhaust hoods. Arbete och Hälsa 34, National Intitute of Occupational Health, Solna, 1989.
30. Garrison RP, Park C and Wang Y. Finite element modeling for velocity characteristics of local exhaust. Inlets, Ventilation '88, Edited by: JH Vincent, Pergamon Press, (1988) 15-24.
31. Heinen H and Zeller M. Numerical calculation of lateral exhaust system for open vessels in industrial application, Third seminar on "Application of Fluid Mechanics in Environmental protection-88", Silesian Technical University, Gliwice, 1988.
32. Braconnier R, Regnier R and Bonthoux F. An experimental and numerical study of the capture of pollutants over a surface-treating tank equipped with a suction slot. In Hughes RT, Goodfellow HD and Rajhaus GS (Ed.). Ventilation '91, Proceedings of the 3rd International Symposium on Ventilation for Contaminant Control. ACGIH, Cincinnati 1993, 95-105.
33. Madsen U. Private communication, Aalborg University, 1994.
34. Fontaine JR, Braconnier R, Rapp K, Sérieys JC. EOL: A computational fluid dynamics software designed to solve air quality problems. In Hughes RT, Goodfellow HD and Rajhaus GS (Ed.). Ventilation '91, Proceedings of the 3rd International Symposium on Ventilation for Contaminant Control. ACGIH, Cincinnati (1993) 95-105.
35. Jansson A. The capture of contaminants by exhausts (In Swedish). Arbete och Hälsa 11, National Institute of Occupational Health, Solna, 1982.
36. Madsen U, Aubertin G, Breum NO, Fontaine JR and Nielsen PV. Tracer gas technique versus a control box method for estimating direct capture efficiency of exhaust systems,. Ventilation '94, Proceedings of the 4th International Symposium on Ventilation for Contaminant Control, Stockholm 1994.